ANTIMICROBIAL AGENTS AND CHEMOTHERAPY, Nov. 2008, p. 3844–3850 Vol. 52, No. 11
0066-4804/08/$08.00+0 doi:10.1128/AAC.00532-08

Genomewide Expression Profiling of Cryptolepine-Induced Toxicity in *Saccharomyces cerevisiae*▽

Marta Rojas,[1] Colin W. Wright,[2] Benjamin Piña,[1] and José Portugal[1]*

Instituto de Biologia Molecular de Barcelona, CSIC, Parc Cientific de Barcelona, E-08028 Barcelona, Spain,[1] and Bradford School of Pharmacy, University of Bradford, West Yorkshire, BD7 1DP, United Kingdom[2]

Received 24 April 2008/Returned for modification 19 July 2008/Accepted 7 August 2008

We have used the budding yeast *Saccharomyces cerevisiae* to identify genes that may confer sensitivity in vivo to the antimalarial and cytotoxic agent cryptolepine. Five *S. cerevisiae* strains, with different genetic backgrounds in cell permeability and DNA damage repair mechanisms, were exposed to several concentrations of cryptolepine. Cryptolepine showed a relatively mild toxicity for wild-type strains, which was augmented by either increasing cell permeability (Δ*erg6* or *ISE2* strains) or disrupting DNA damage repair (Δ*rad52* strains). These results are compatible with the ability of cryptolepine to intercalate into DNA and thus promote DNA lesions. The effects of low concentrations of cryptolepine (20% and 40% inhibitory concentrations [IC_{20} and IC_{40}]) were analyzed by comparing the gene expression profiles of treated and untreated Δ*erg6* yeast cells. Significant changes in expression levels were observed for 349 genes (117 upregulated and 232 downregulated). General stress-related genes constituted the only recognizable functional cluster whose expression was increased upon cryptolepine treatment, making up about 20% of upregulated genes. In contrast, analysis of the characteristics of downregulated genes revealed a specific effect of cryptolepine on genes related to iron transport or acid phosphatases, as well as a significant proportion of genes related to cell wall components. The effects of cryptolepine on the transcription of iron transport-related genes were consistent with a loss of function of the iron sensor Aft1p, indicating a possible disruption of iron metabolism in *S. cerevisiae*. Since the interference of cryptolepine with iron metabolism is considered one of its putative antimalarial targets, this finding supports the utility of *S. cerevisiae* in drug-developing schemes.

Cryptolepine is the main indoloquinoline alkaloid found in the roots of the climbing shrub *Cryptolepis sanguinolenta* (Periplocaceae). In West Africa, decoctions of the roots of *C. sanguinolenta* are used in traditional medicine to treat malaria as well as a variety of other infectious diseases (27). Cryptolepine (Fig. 1) has shown in vitro antiplasmodial activity (27), but this alkaloid also has cytotoxic properties in several cell lines, and the mechanisms involved may include intercalation into DNA, as well as inhibition of topoisomerase II and DNA synthesis (4). The mode of cryptolepine intercalation into DNA is peculiar in that it occurs at nonalternating C/G sequences (12).

Regardless of the binding of cryptolepine to DNA (3, 12), investigations into its molecular mechanisms of action have revealed that the antiplasmodial mode of action may be different from the cytotoxic mode of action. Cryptolepine shares with chloroquine, and related quinoline antimalarial drugs, the property of binding to heme and prevents its conversion to hemazoin (28). The drug-heme complex is considered to be toxic to the parasite.

Deeper knowledge of the different targets of cryptolepine should help to elucidate the basis for the relative selectivity of this alkaloid against malaria parasites and should assist in the rational development of cryptolepine derivatives with enhanced antimalarial activities. The antimalarial activity of cryptolepine is considered to be pleiotropic rather than dependent on a unique mechanism. It may encompass many different pathways, including binding to DNA, transcriptional inhibition of certain genes, formation of drug-heme complexes, and its accumulation in the parasite food vacuole (where hemoglobin digestion takes place) and in other organelles (25, 27). Valuable insights into determinants of virulence, drug responses, and cellular development in population structures of human malaria parasites can be facilitated by the ongoing sequencing of the *P. falciparum* genome (9) (available at the *Plasmodium falciparum* Genome Database [http://www.tigr.org/tdb/edb2/pfa1/htmls/]). A detailed understanding of the molecular bases of drug response can be further facilitated by using simpler model organisms, such as the budding yeast *Saccharomyces cerevisiae*, the genome of which is fully annotated and widely characterized (available at the *Saccharomyces* Genome Database [SGD] [http://www.yeastgenome.org/]). This eukaryotic model organism has proven to be a powerful genetic system for testing drugs that can interact with DNA and/or modify gene regulation, since it shares many common regulatory mechanisms with vertebrates, ranging from cell cycle to transcriptional regulation (14–16, 30).

To gain new insights into the role played by changes in the transcriptome during exposure to cryptolepine, we have undertaken a genomewide analysis using *S. cerevisiae* to identify genes responsive to this drug. The main drawback of the use of yeast in pharmacological studies is its resistance to many drugs (15, 16), which is due to the strict permeability barrier formed by the yeast cellular membrane. In a previous paper, we have shown that yeast strains deficient in ergosterol synthesis (Δ*erg6* strains) are particularly sensitive to the antitumor antibiotic

* Corresponding author. Mailing address: Instituto de Biología Molecular de Barcelona, CSIC, Parc Científic de Barcelona, Baldiri Reixach, 10, E-08028 Barcelona, Spain. Phone: 34-93-403 4959. Fax: 34-93-403 4979. E-mail: jpmbmc@ibmb.csic.es.

▽ Published ahead of print on 18 August 2008.

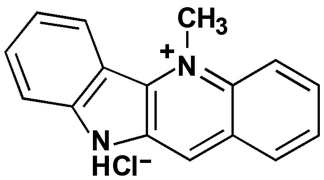

FIG. 1. Chemical structure of cryptolepine hydrochloride.

daunorubicin (14). In the Δ*erg6* background, we also demonstrated the specific inhibition of genes involved in galactose utilization by daunorubicin, and we suggested that this was related to the presence of CpG steps in the recognition sequence of the main regulator for these genes, Gal4p (14). Here we extend these studies to the antimalarial drug cryptolepine by using the whole budding yeast transcriptome. We observed specific changes in the transcriptome, rather than a general malfunction of the transcriptional network. These results are consistent with those observed in the transcription profiles produced by other DNA-binding drugs in different cell types, including *S. cerevisiae* (2, 10, 13, 21), and provide us with some clues on the peculiar characteristics of cryptolepine effects in vivo. From the analysis of transcriptional profiles, we found that cryptolepine induced specific inhibition of several genes, mainly genes involved in stress response and iron usage. Many of the affected genes were controlled by Aft1p, the major iron-dependent transcription factor in *S cerevisiae* (22). The similarities between transcriptome changes induced by cryptolepine and those resulting from Aft1p loss of function suggest a mechanism of disruption of iron uptake and/or signaling for at least part of the cytotoxicity of cryptolepine. This effect may be central to understanding of the mechanisms underlying cryptolepine sensitivity in both *S. cerevisiae* and *Plasmodium* spp.

MATERIALS AND METHODS

Cryptolepine preparation. Cryptolepine was isolated and purified as the hydrochloride salt from *C. sanguinolenta* as described elsewhere (29). It was freshly prepared as a 1 mM stock solution in methanol and diluted to final concentrations before use.

Yeast strains and growth assays. The following strains of *Saccharomyces cerevisiae* were used: BY4741 (*MAT***a** *his3Δ1 leu2Δ0 met15Δ0 ura3Δ0*) and its derived single deletion mutant strains BY4741Δ*erg6* (*erg6*::*KanMX4*) and BY4741Δ*rad52* (*rad52*::*KanMX4*), available through EUROSCARF (Frankfurt, Germany). Permeable yeast strains JN362a (*MAT***a** *ura3-52 leu2 trp1 his7 ade1 ISE2*) and JN394 (JN362a *rad52*::*LEU2*) (15) were obtained from J. Roca (IBMB-CSIC, Barcelona, Spain).

The different yeast strains were precultured in complete YPD medium (10 g/liter yeast extract, 20 g/liter peptone, and 20 g/liter dextrose) at 30°C for 15 h with shaking at 250 rpm in the dark. Before the strains were used for the different experiments, the number of cells was standardized (optical density at 600 nm [OD_{600}], 0.05) using the same medium. Yeast was grown in triplicate in 96-well microtiter plates in the same medium in the presence of different concentrations of cryptolepine. Yeast growth was measured as OD_{600} units.

RNA preparation. Cultures were centrifuged for 5 min at 3,000 rpm, washed with 5 ml MilliQ water, and subsequently centrifuged (the whole procedure was repeated twice). Total RNA was extracted with the RiboPure yeast kit (Ambion, Austin, TX) and quantified by spectrophotometry using a NanoDrop ND-1000 spectrophotometer (NanoDrop Technologies, Wilmington, DE), and its integrity was checked on agarose gels. The resulting total RNA was then treated with DNase I (F. Hoffmann-La Roche, Basel, Switzerland) to remove any genomic DNA.

DNA microarray analysis. Yeast genomic microchips were constructed in the Institute of Biology and Biotechnology, Autonomous University of Barcelona, Barcelona, Spain, by arraying 6,014 different PCR-amplified open reading frames (ORFs) from *S. cerevisiae* (26). Fifteen micrograms of total RNA, isolated as described above, was used for cDNA synthesis and labeling with Cy3-dUTP and Cy5-dUTP fluorescent nucleotides by following an indirect labeling protocol (CyScribe postlabeling kit; GE-Healthcare, New York, NY). Labeling efficiency was evaluated by spectrophotometric measurement of Cy3 or Cy5 absorbance. Microarray prehybridization was performed in 5× SSC (1× SSC is 0.15 M NaCl plus 0.015 M sodium citrate [pH 7.0])–0.1% sodium dodecyl sulfate–1% bovine serum albumin at 42°C for 45 min. Labeled cDNA was dried in a vacuum trap and used as a probe after resuspension in 110 μl of hybridization solution (50% formamide, 5× SSC, 0.1% sodium dodecyl sulfate, 100 μg/ml salmon sperm DNA). Hybridization and washing were performed in a Lucidea Slide Pro system (GE Healthcare, Uppsala, Sweden). Arrays were scanned with a GenePix 4000B fluorescence scanner and analyzed by Genepix 5.0 Pro software (Axon Instruments, MDS Analytical Technologies, Toronto, Ontario, Canada). Only spots whose intensity was 1.5 times that of the background signal were selected for further calculations. Eight sets of microarray data are presented here, corresponding to treatments with two different cryptolepine concentrations (7.5 and 17 μM, equivalent to 20% and 40% inhibitory concentrations [IC_{20} and IC_{40}], respectively), each performed in duplicate. Each RNA preparation was labeled and hybridized twice, and dyes were swapped between treated and untreated samples. Data are presented as fluorescence ratios of treated versus untreated cell cultures.

qRT-PCR assay. An aliquot of RNA preparations from untreated and treated samples, used in the microarray experiments, was used for quantitative real-time reverse transcriptase PCR (qRT-PCR) follow-up studies. Two additional biological replicates were performed as described above. First-strand cDNAs were synthesized from 2 μg of total, DNase I-treated RNA in a 20-μl reaction volume using the Omniscript RT kit (Qiagen, Valencia, CA) according to the manufacturer's instructions. qRT-PCRs were performed in triplicate using the ABI Prism 7000 sequence detection system (Applied Biosystems, Foster City, CA) with the Sybr green PCR master mix (Applied Biosystems). Gene-specific primers were designed using Primer Express software (Applied Biosystems); primer sequences are listed in Table 1. Amplified fragments were confirmed by sequencing in an Applied Biosystems 3730 DNA analyzer, and the sequences were compared with the genomic data published at the SGD. PCR conditions included an initial denaturation step at 95°C for 10 min, followed by 40 cycles of a denaturation step at 95°C for 15 s and an annealing/extension step at 60°C for 1 min. A final dissociation curve was generated to verify that a single product was amplified. A series of 10-fold dilutions of genomic DNA covering a total dilution range from 1 to 10^{-6} was used to generate the standard curves. Genomic DNA was purified using a MasterPure yeast DNA purification kit (Epicentre) according to the manufacturer's protocol. Reactions in the absence of template and in the absence of enzyme were also performed in triplicate for each primer pair as negative controls. The relative expression values of different genes were calculated from the threshold cycle (C_T) by the $\Delta\Delta C_T$ method (17).

Data analysis. Dual logarithmic values of the ratios of fluorescence rates for cryptolepine-treated versus untreated cells were used for subsequent analysis. Because no significant differences were found between cells treated with 7.5 versus 17 μM concentrations of cryptolepine (see below), the eight sets of microarray data were considered equivalent and used accordingly. Differences in fluorescence rates between treated and untreated cells for each ORF were considered significant when the probability of the corresponding ratios being equal to 1 was below 0.01 (two-tailed Student *t* test with logarithm-transformed data from the eight hybridizations). Genes were classified by gene ontology (GO) in the biological-process category (5) at the SGD page (http://www.yeastgenome.org/).

Microarray data accession number. The entire set of microarray data has been deposited in the GEO (Gene Expression Omnibus) database (http://www.ncbi.nlm.nih.gov/projects/geo/) under accession number GSE12192.

RESULTS

Sensitivity of *S. cerevisiae* to cryptolepine. Figure 2 shows the results of assays of yeast cell growth in the presence of different concentrations of cryptolepine. The data presented correspond to experiments consisting of continuous treatments of the different yeast strains for 4 h. Cell growth was determined as described in Materials and Methods, and the IC_{40}s calculated from the plots can be seen in Fig. 2. We selected this rather mildly inhibitory condition to ensure that the effects of the drug on the yeast transcriptome were not a direct consequence

TABLE 1. Sequences of primers used for qRT-PCR assays

Gene and primer	Primer sequence	Gene function
ACT1		Actin
for	5′-TGTGTAAAGCCGGTTTTGCC-3′	
rev	5′-TTGACCCATACCGACCATGAT-3′	
ARN2		ARN transporter family; recognizes siderophore-iron chelates
for	5′-CGTGGAATGGAAAGAATTACAGG-3′	
rev	5′-CCGTGCGTTTGATAGTACGATTT-3′	
FIT3		Mannoprotein, involved in the retention of siderophore iron in the cell wall
for	5′-TGTCTGGACTGGTGAAGGCAG-3′	
rev	5′-GAAGTACTACTTGGAGACCAGGTGTTG-3′	
TIS11		mRNA-binding protein, involved in iron homeostasis
for	5′-TCGGCAGTTTCATTCTCTCCA-3′	
rev	5′-CCCCGGTTGAATAGCGTTT-3′	
TPS1		Synthase subunit of trehalose-6-phosphate synthase/phosphatase complex
for	5′-CGACGAGAATGCGTGGTTG-3′	
rev	5′-TTGGTGAACGTCTGGTTTGC-3′	
PHO5		Repressible acid phosphatase
for	5′-CATGCTCGTGACTTCTTGGC-3′	
rev	5′-GGTTTGGTTTTCGACCATGTAAC-3′	
HSP26		Small heat shock protein (sHSP) with chaperone activity
for	5′-AGAGGCTACGCACCAAGACG-3′	
rev	5′-AGAATCCTTTGCGGGTGTGT-3′	

of a general cytotoxic effect but more-direct, and somewhat specific, effects on transcriptional levels; thus, this concentration was used in experiments aimed at isolating RNAs after longer incubation times.

The most sensitive yeast strain was JN394 (*ISE2* Δ*rad52*) (IC_{50}, 20.29 ± 1.77 μM), followed by BY4741Δ*erg6* (IC_{50}, 25.03 ± 4.87 μM). These results would indicate that damage/repair mechanisms, together with cell permeability, are involved in the toxicity of cryptolepine. To reduce the growth of strain JN362a by 50% required a concentration almost twice that required for the BY4741Δ*erg6* strain, whereas the JN394 *ISE2* strain was twofold more sensitive than the isogenic strain JN362a (Fig. 2). Since *RAD52* function is central for DNA repair by homologous recombination, this result suggests that cryptolepine affects DNA repair mechanisms, in keeping with the ability of cryptolepine to intercalate into DNA and trigger genetic damage (1).

At cryptolepine concentrations below 10 μM, higher sensitivity was observed for the BY4741Δ*erg6* strain, despite its *RAD52* wild-type background (Fig. 2). Because we intended to

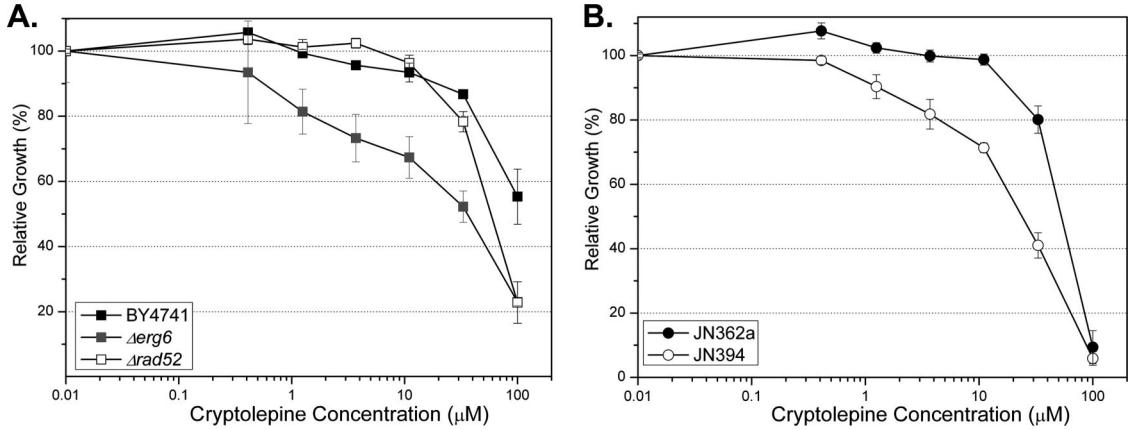

FIG. 2. Effects of cryptolepine on the cell growth of different *Saccharomyces cerevisiae* strains deficient in specific genes or combinations of genes. (A) Effects of cryptolepine on the wild-type strain BY4741 and its derived mutant strains BY4741Δ*erg6* and BY4741Δ*rad52*. (B) Effects on the *ISE2* strain JN362a and its Δ*rad52* derivative JN394. Each data point represents the percentage of relative growth (drug-treated compared to control cells) versus the concentration of cryptolepine in the growth medium. Data are means ± standard deviations from three independent experiments.

TABLE 2. GO terms associated with genes significantly[a] up- or downregulated by cryptolepine

Criterion	GO term	Cluster frequency[b]	Background frequency[b]	*P*	Genes annotated to the term
Downregulated genes					
Process	Siderophore transport	6/231 (2.6)	9/7,156 (0.1)	3.87×10^{-5}	*FIT1*, *SIT1*, *ARN1*, *ARN2*, *FIT2*, *FIT3*
	Glucose catabolic process	8/231 (3.5)	26/7,156 (0.4)	4.6×10^{-4}	*CDC19*, *PGK1*, *HXK2*, *ENO2*, *GND1*, *PFK2*, *RKI1*, *TKL1*
Function	Acid phosphatase activity	4/231 (1.7)	5/7,155 (0.1)	7.4×10^{-4}	*PHO11*, *PHO3*, *PHO5*, *PHO12*
Component	Fungal-type cell wall	18/231 (7.8)	91/7,156 (1.3)	6.7×10^{-8}	*FLO9*, *FLO1*, *ECM33*, *PHO5*, *TOS1*, *DAN3*, *EXG2*, *FIT1*, *TIR1*, *CIS3*, *DAN1*, *PLB2*, *EGT2*, *GAS5*, *TIR4*, *TIR2*, *FIT2*, *FIT3*
Upregulated genes					
Process	Response to stress	23/117 (19.7)	487/7,156 (6.8)	7.7×10^{-4}	*SSA1*, *UGA2*, *HSP26*, *UBC4*, *TPS1*, *HSP30*, *HSP42*, *SSA4*, *HSP12*, *RAD6*, *ERV1*, *CTT1*, *ZPR1*, *GRE3*, YJL144W, *CCP1*, *HSP104*, *TSL1*, *ALD3*, *HOR7*, *NCE103*, *YGP1*, *RFC4*
Function	No significant ontology term[c]				
Component	No significant ontology term[c]				

[a] At a *P* value of <0.01.
[b] Expressed as the number of genes/total genes (percentage).
[c] $P < 10^{-3}$.

identify toxic effects independent of DNA damage, we used this strain to analyze the effects of moderately cytotoxic concentrations (IC_{20} and IC_{40}) of cryptolepine in the transcriptome of *S. cerevisiae*.

Effects of cryptolepine on the yeast transcriptome. Expression data from yeast cells treated with 7.5 or 17 μM cryptolepine (the IC_{20} and IC_{40}, respectively) and untreated cells were compared after 15-h treatments. No significant differences were found between the two treatments ($P < 0.05$ by Student's *t* test). Of 4,416 genes whose expression was correctly quantified (73% of printed ORFs), 349 genes (8%) showed statistically significant differences in expression between cryptolepine-treated and untreated cells; of these, 117 genes showed higher expression in treated cells and 232 appeared to be downregulated by cryptolepine. Twenty-three of 117 genes activated upon cryptolepine treatment were included in the functional class of "response to stress" by GO analysis (Table 2); this was the only functional class detected for upregulated genes by this analysis. Upregulated genes included five *HSP* genes and two genes involved in trehalose synthesis (*TSL1* and *TPS1*), a typical response of yeast to general stress conditions (7).

GO analysis of downregulated genes showed several well-defined functional gene categories (Table 2). This subset of genes included six of the nine genes involved in siderophore transport; the expression levels of the remaining three genes were too low to permit their precise quantification in the arrays. Similarly, the four repressible yeast acid phosphatases (*PHO3*, *PHO5*, *PHO11*, and *PHO12*) appeared to be downregulated upon cryptolepine treatment. A significant portion of downregulated genes (8%; $P = 6.7 \times 10^{-8}$) (Table 2) corresponded to elements of the cell wall, suggesting a specific action of cryptolepine on this structure. Finally, a small but significant portion of downregulated genes was related to the glycolytic and pentose phosphate pathways (Table 2). The pentose phosphate metabolic pathway is known to participate in the protective response to oxidative stress in yeast (23).

Cryptolepine-induced changes in the expression of genes belonging to each of the functional categories mentioned above were corroborated by qRT-PCR (Table 3). The results from qRT-PCR and microarrays were essentially identical, except for an apparent underestimation of the repression levels for some genes by microarray analysis. There were no significant differences between cells treated with 7.5 versus 17 μM cryptolepine (Table 3). Therefore, these combined data indicated decreases in the expression of siderophore transport and acid phosphatase genes, and enhancement of the expression of stress-related genes, as a consequence of cryptolepine treatment.

Effects of cryptolepine on Aft1p-regulated genes. The set of genes regulated by Aft1p, the so-called Aft1p regulon, has been determined previously by analyzing the transcriptional differences between Aft1p-deficient (Δ*aft1*) cells and cells carrying the constitutively activated AFT1-1^{up} allele (22). We compared these results with our data on the effects of cryptolepine on Δ*erg6* yeast cells. Both data sets showed little or no correlation for most genes, except for a defined subset that corresponds to the iron transport-related genes (Fig. 3). The expression of these genes is strongly dependent on Atf1p (22), which was downregulated upon cryptolepine treatment. Figure

TABLE 3. Cryptolepine-induced changes in the expression of several genes calculated from microarray and qRT-PCR results

Gene	Log_2-transformed gene expression ratio[a] for cells treated with cryptolepine at the following concn relative to untreated cells:			
	7.5 μM		17 μM	
	Microarray	qRT-PCR	Microarray	qRT-PCR
ARN2	−2.18	−4.06	−3.32	−4.90
FIT3	−3.30	−5.57	−2.36	−2.01
PHO5	−1.88	−1.73	−2.05	−2.27
TIS11	−2.35	−3.30	−2.31	−3.46
HSP26	2.09	2.49	3.54	3.51
TPS1	1.24	0.96	1.01	1.03

[a] Minus signs indicate downregulation. Data are averages from duplicate experiments for each treatment.

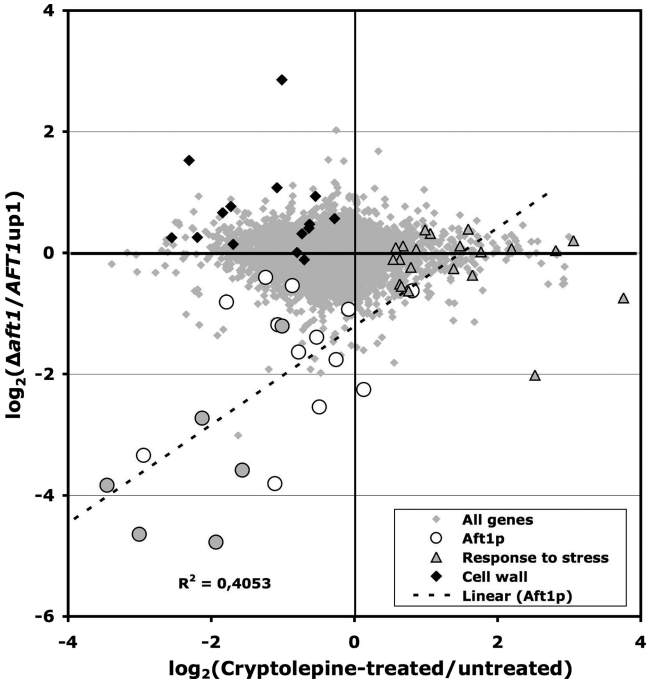

FIG. 3. Comparison of changes in transcription rates induced by cryptolepine treatment (*x* axis) with those related to Aft1p activity (*y* axis). The plot shows two sets of microarray results, both presented as dual logarithms of relative transcription rates. The *y* axis includes data from reference 22 and compares the transcriptome from the Δ*aft1* yeast strain to that of an isogenic strain carrying the constitutively activated *AFT1-1*^{up} allele. The *x* axis represents average expression ratios for cryptolepine-treated versus untreated cells; all treatments and replicates discussed in the text are included. Genes identified as implicated in iron uptake, whose names are given in Table 4, are represented by circles. The correlation between the two data sets for the iron uptake-related genes (some of which are included in Table 2) is represented by the corresponding regression line; the correlation coefficient is also given on the graph. Genes involved in stress, which correspond to the two major categories affected by cryptolepine as indicated in Table 2 (cell wall and stress response genes), are also shown.

3 also shows several genes grouped under the "response to stress" and "fungal-type cell wall" categories, the other two large functional subsets of genes affected by cryptolepine treatment (see Table 2). For these functional categories, no correlation was observed between the effects of cryptolepine treatment and Aft1p function.

The effects of cryptolepine on genes related to iron transport are further detailed in Table 4. This table shows all genes that have been related to iron uptake processes for which we obtained data on the effects of cryptolepine treatment. The genes were classified by the iron uptake pathway to which they are related (11) and by their functions (Table 4). Genes of the siderophore-related pathway were particularly sensitive to cryptolepine. In addition, the transcription of some genes belonging to other iron uptake pathways was also significantly downregulated. Table 4 also shows that there was a good correlation between cryptolepine-affected genes and Aft1p-dependent genes, with some exceptions (notably *FRE3* and *FRE6*). We conclude that cryptolepine affects genes involved in iron uptake in yeast, especially those related to the siderophore-dependent pathway and that, in general, the expression profile coincided with the requirement for Aft1p for the transcription of these genes.

DISCUSSION

The morbidity and mortality associated with malaria have encouraged efforts to find novel antimalarial agents with improved potency and selectivity, which include explorations of cryptolepine and some derivatives (25, 27, 28). In this context, we have examined changes in the gene expression profile of the budding yeast *S. cerevisiae* induced by low doses of cryptolepine in order to gain new insights into its mechanisms of action. By using rather mild conditions, we were able to examine the effects of this antimalarial drug under conditions under which its general cytotoxicity was very much reduced. Three functional subsets of genes changed their expression levels significantly upon exposure to cryptolepine: general stress genes, which became activated, and cell wall components and iron transport genes, which became repressed. These effects occurred at much lower concentrations than those required for DNA damage-mediated toxicity and may correlate with the effects of cryptolepine on plasmodia.

In general, eukaryotic cells respond to DNA damage by arresting the cell cycle and modulating gene expression to ensure efficient DNA repair. Various yeast genes involved in cell cycle arrest after DNA damage are homologous to repair genes in humans (8). The effects of cryptolepine on repair genes agree with the higher sensitivity of Δ*rad52* yeast strains to cryptolepine in assays of growth sensitivity to the drug (Fig. 2), indicating that DNA damage is a key factor in the mechanism of cryptolepine cytotoxicity. The results presented here are relevant to the pursuit of new cryptolepine derivatives with reduced toxicity; for cryptolepine, toxicity is usually attributed to its binding to DNA (28). Intriguingly, cryptolepine binds preferentially to C/G-rich DNA tracts (3, 12); these sequences are underrepresented in the *P. falciparum* genome, which contains about 80% A+T DNA and therefore a lower number of potential binding sites than other organisms. Cryptolepine intercalates into DNA (12), and it also inhibits topoisomerase II (3, 4). However, this inhibition has been suggested to play a minor role in cytotoxicity (4). Therefore, DNA damage may be an indirect consequence of treatment with this drug, since several genes involved in genetic recombination displayed altered patterns of expression after cryptolepine treatment.

The remarkable flexibility of yeast in the use of iron and other essential nutrients is not completely understood (18), although iron may be involved in triggering the activation of some genes. Our results indicate that the expression of a representative set of genes involved in iron metabolism, particularly in siderophore-iron complex uptake, is dramatically changed by cryptolepine (Table 4), a molecule that has been documented to alter iron usage in other organisms (20). Data mining revealed that the transcription of iron transport-related genes was altered by cryptolepine, following a pattern similar to that observed for Aft1p-deficient cells compared to Aft1-activated cells. Aft1p is the major regulon responsible for the remodeling of the yeast transcriptome under conditions of iron deprivation (22). Lack of Atf1p function results in the inability of the cell to adapt its metabolism to changes in iron availabil-

TABLE 4. Aft1p dependence of *S. cerevisiae* iron transport genes and their inhibition by cryptolepine

Iron uptake pathway[a] and function	Affinity[a,b]	Gene name	Systematic name	Log_2-transformed gene expression ratio[c] for:	
				Cryptolepine-treated/ untreated cells	Δ*aft1*/AFT1-1^{up} cells[d]
Siderophore dependent					
Facilitator, Fe(III) complex	H	*ARN1*	YHL040C	−1.07	−1.19
	H	*ARN2*	YHL047C	−3.01	−4.64
	H	*SIT1*	YEL065W	−1.57	−3.58
Retention of siderophore-iron complexes to membrane	H	*FIT1*	YDR534C	−2.13	−2.72
	H	*FIT2*	YOR382W	−1.94	−4.77
	H	*FIT3*	YOR383C	−3.46	−3.84
Reductase/ferroxidase dependent					
Reductases, Fe(III) and Cu(II), free or complexed	H	*FRE1*	YLR214W	−0.78	−1.64
	H	*FRE2*	YKL220C	0.13	−2.26
	H	*FRE5*	YOR384W	−1.01	−1.21
	H	*FRE6*	YLL051C	−0.08	−0.93
Ferroxidases, free Fe(II)	H	*FET3*	YMR058W	−1.11	−3.81
	H	*FET5*	YFL041W	0.80	−0.63
Reductase/permease dependent					
Permeases, ferroxidase-generated Fe(III)	H	*FTR1*	YER145C	−0.49	−2.54
	H	*FTH1*	YBR207W	−0.53	−1.39
	L	*FET4*	YMR319C	−1.79	−0.81
Permeases, ferroxidase-generated Fe(III) and Mn(II)	L	*SMF1*	YOL122C	−0.35	0.42
	L	*SMF2*	YHR050W	0.09	0.16
	L	*SMF3*	YLR034C	−1.24	−0.40

[a] Data from reference 11.
[b] H, high affinity (K_m, <2 μM); L, low affinity (K_m, >2 μM).
[c] Minus signs indicate downregulation.
[d] Data from reference 22.

ity and to regulate different cellular processes (22, 24). Whereas these effects produce only relatively mild growth defects in a facultative respirator such as *S. cerevisiae*, the changes observed in the yeast transcriptome may uncover the molecular origin of cryptolepine's activity against *Plasmodium* spp.

Iron assimilation seems to be a common theme in the mechanism of several antimalarial drugs. Millimolar concentrations of chloroquine can prevent iron uptake in yeast (6), resulting in the upregulation of Aft1p-regulated genes and growth defects under iron-limiting conditions. The apparently opposite effect of micromolar concentrations of cryptolepine on the same regulon should have a synergistic effect, because the combination of low expression of iron-assimilating genes and prevention of iron assimilation would produce a very severe effect on the oxidative metabolism of the affected cells. Whether this cumulative effect occurs in plasmodia remains to be elucidated.

Although experimental evidence supports a high degree of conservation of the major signaling pathways and basic cellular processes among simple eukaryotic organisms (16), the occurrence of homology and/or orthology among *S. cerevisiae* and *P. falciparum* genes involved in iron usage and metabolism and in stress response is not, at present, straightforward to establish, owing to the fact that sequencing of the *P. falciparum* genome is ongoing (9). A search among the genes listed in Table 2 failed to produce definitive evidence of orthology between the iron usage genes in *S. cerevisiae* and *P. falciparum*. Nevertheless, some of those genes are orthologous in humans; thus, depletion of iron genes may interfere with labile iron stores in both host human cells and *Plasmodium* spp. (18).

Notwithstanding the binding of cryptolepine to DNA, the main effect of the drug in yeast was clearly on stress response. This is at variance with our analysis of the effect of the DNA-binding antitumor antibiotic daunorubicin using microarrays, which showed a stronger effect on the control of gene transcription in the yeast Δ*erg6* strain (19). Taken together, these transcriptomewide studies would indicate that it is feasible to separate the cytotoxic effect provided by DNA binding from other pathways that may be ascribed to the antiplasmodial activity of cryptolepine, such as iron usage. This observation may be used in the pursuit of improved molecules related to cryptolepine, which might hopefully separate those effects (28) even more clearly than we have described here, through a genomewide analysis of *S. cerevisiae*.

ACKNOWLEDGMENTS

This work has been supported by grants from the former Spanish Ministry of Education and Science (BIO2005-00840, BFU2007-60998/BMC, and AGL2000-0133-P4-03). The contribution of the Centre de Referencia en Biotecnologia of the Generalitat de Catalunya is also acknowledged.

REFERENCES

1. **Ansah, C., A. Khan, and N. J. Gooderham.** 2005. In vitro genotoxicity of the West African anti-malarial herbal *Cryptolepis sanguinolenta* and its major alkaloid cryptolepine. Toxicology **208:**141–147.
2. **Benton, M. G., S. Somasundaram, J. D. Glasner, and S. P. Palecek.** 2006. Analyzing the dose-dependence of the *Saccharomyces cerevisiae* global transcriptional response to methyl methanesulfonate and ionizing radiation. BMC Genomics **7:**305.
3. **Bonjean, K., M. C. De Pauw-Gillet, M. P. Defresne, P. Colson, C. Houssier, L. Dassonneville, C. Bailly, R. Greimers, C. Wright, J. Quetin-Leclercq, M. Tits, and L. Angenot.** 1998. The DNA intercalating alkaloid cryptolepine interferes with topoisomerase II and inhibits primarily DNA synthesis in B16 melanoma cells. Biochemistry **37:**5136–5146.
4. **Dassonneville, L., A. Lansiaux, A. Wattelet, N. Wattez, C. Mahieu, S. Van Miert, L. Pieters, and C. Bailly.** 2000. Cytotoxicity and cell cycle effects of the plant alkaloids cryptolepine and neocryptolepine: relation to drug-induced apoptosis. Eur. J. Pharmacol. **409:**9–18.
5. **Dwight, S. S., M. A. Harris, K. Dolinski, C. A. Ball, G. Binkley, K. R. Christie, D. G. Fisk, L. Issel-Tarver, M. Schroeder, G. Sherlock, A. Sethuraman, S. Weng, D. Botstein, and J. M. Cherry.** 2002. *Saccharomyces* Genome Database (SGD) provides secondary gene annotation using the Gene Ontology (GO). Nucleic Acids Res. **30:**69–72.
6. **Emerson, L. R., M. E. Nau, R. K. Martin, D. E. Kyle, M. Vahey, and D. F. Wirth.** 2002. Relationship between chloroquine toxicity and iron acquisition in *Saccharomyces cerevisiae*. Antimicrob. Agents Chemother. **46:**787–796.
7. **Estruch, F.** 2000. Stress-controlled transcription factors, stress-induced genes and stress tolerance in budding yeast. FEMS Microbiol. Rev. **24:**469–486.
8. **Gasch, A. P., M. Huang, S. Metzner, D. Botstein, S. J. Elledge, and P. O. Brown.** 2001. Genomic expression responses to DNA-damaging agents and the regulatory role of the yeast ATR homolog Mec1p. Mol. Biol. Cell **12:**2987–3003.
9. **Hoffman, S. L., G. M. Subramanian, F. H. Collins, and J. C. Venter.** 2002. *Plasmodium*, human and *Anopheles* genomics and malaria. Nature **415:**702–709.
10. **Jelinsky, S. A., and L. D. Samson.** 1999. Global response of *Saccharomyces cerevisiae* to an alkylating agent. Proc. Natl. Acad. Sci. USA **96:**1486–1491.
11. **Kosman, D. J.** 2003. Molecular mechanisms of iron uptake in fungi. Mol. Microbiol. **47:**1185–1197.
12. **Lisgarten, J. N., M. Coll, J. Portugal, C. W. Wright, and J. Aymamí.** 2002. The antimalarial and cytotoxic drug cryptolepine intercalates specifically to DNA at cytosine-cytosine sites. Nat. Struct. Biol. **9:**57–60.
13. **Mansilla, S., B. Piña, and J. Portugal.** 2003. Daunorubicin-induced variations in gene transcription: commitment to proliferation arrest, senescence and apoptosis. Biochem. J. **372:**703–711.
14. **Marín, S., S. Mansilla, N. Garcia-Reyero, M. Rojas, J. Portugal, and B. Piña.** 2002. Promoter-specific inhibition of transcription by daunorubicin in *Saccharomyces cerevisiae*. Biochem. J. **368:**131–136.
15. **Nitiss, J., and J. C. Wang.** 1988. DNA topoisomerase-targeting antitumor drugs can be studied in yeast. Proc. Natl. Acad. Sci. USA **85:**7501–7505.
16. **Perego, P., G. S. Jimenez, L. Gatti, S. B. Howell, and F. Zunino.** 2000. Yeast mutants as a model system for identification of determinants of chemosensitivity. Pharmacol. Rev. **52:**477–492.
17. **Pfaffl, M. W.** 2001. A new mathematical model for relative quantification in real-time RT-PCR. Nucleic Acids Res. **29:**e45.
18. **Philpott, C. C., and O. Protchenko.** 2008. Response to iron deprivation in *Saccharomyces cerevisiae*. Eukaryot. Cell **7:**20–27.
19. **Rojas, M., M. Casado, J. Portugal, and B. Piña.** 2008. Selective inhibition of yeast regulons by daunorubicin: a transcriptome-wide analysis. BMC Genomics **9:**358.
20. **Sawer, I. K., M. I. Berry, and J. L. Ford.** 2005. The killing effect of cryptolepine on *Staphylococcus aureus*. Lett. Appl. Microbiol. **40:**24–29.
21. **Scherf, U., D. T. Ross, M. Waltham, L. H. Smith, J. K. Lee, L. Tanabe, K. W. Kohn, W. C. Reinhold, T. G. Myers, D. T. Andrews, D. A. Scudiero, M. B. Eisen, E. A. Sausville, Y. Pommier, D. Botstein, P. O. Brown, and J. N. Weinstein.** 2000. A gene expression database for the molecular pharmacology of cancer. Nat. Genet. **24:**236–244.
22. **Shakoury-Elizeh, M., J. Tiedeman, J. Rashford, T. Ferea, J. Demeter, E. Garcia, R. Rolfes, P. O. Brown, D. Botstein, and C. C. Philpott.** 2004. Transcriptional remodeling in response to iron deprivation in *Saccharomyces cerevisiae*. Mol. Biol. Cell **15:**1233–1243.
23. **Slekar, K. H., D. J. Kosman, and V. C. Culotta.** 1996. The yeast copper/zinc superoxide dismutase and the pentose phosphate pathway play overlapping roles in oxidative stress protection. J. Biol. Chem. **271:**28831–28836.
24. **Steinmetz, L. M., C. Scharfe, A. M. Deutschbauer, D. Mokranjac, Z. S. Herman, T. Jones, A. M. Chu, G. Giaever, H. Prokisch, P. J. Oefner, and R. W. Davis.** 2002. Systematic screen for human disease genes in yeast. Nat. Genet. **31:**400–404.
25. **Van Miert, S., T. Jonckers, K. Cimanga, L. Maes, B. Maes, G. Lemiere, R. Dommisse, A. Vlietinck, and L. Pieters.** 2004. In vitro inhibition of beta-haematin formation, DNA interactions, antiplasmodial activity, and cytotoxicity of synthetic neocryptolepine derivatives. Exp. Parasitol. **108:**163–168.
26. **Viladevall, L., R. Serrano, A. Ruiz, G. Domenech, J. Giraldo, A. Barceló, and J. Ariño.** 2004. Characterization of the calcium-mediated response to alkaline stress in *Saccharomyces cerevisiae*. J. Biol. Chem. **279:**43614–43624.
27. **Wright, C. W.** 2007. Recent developments in naturally derived antimalarials: cryptolepine analogues. J. Pharm. Pharmacol. **59:**899–904.
28. **Wright, C. W., J. Addae-Kyereme, A. G. Breen, J. E. Brown, M. F. Cox, S. L. Croft, Y. Gokcek, H. Kendrick, R. M. Phillips, and P. L. Pollet.** 2001. Synthesis and evaluation of cryptolepine analogues for their potential as new antimalarial agents. J. Med. Chem. **44:**3187–3194.
29. **Wright, C. W., J. D. Phillipson, S. O. Awe, G. C. Kirby, D. C. Warhurst, J. Quetin-Leclercq, and L. Angenot.** 1996. Antimalarial activity of cryptolepine and some other anhydronium bases. Phytother. Res. **10:**361–363.
30. **Wu, H. I., J. A. Brown, M. J. Dorie, L. Lazzeroni, and J. M. Brown.** 2004. Genome-wide identification of genes conferring resistance to the anticancer agents cisplatin, oxaliplatin, and mitomycin C. Cancer Res. **64:**3940–3948.